Research Square

Preprints are preliminary reports that have not undergone peer review.
They should not be considered conclusive, used to inform clinical practice,
or referenced by the media as validated information.

Early Immune Dysregulation Emerges During the Advanced Adenoma–Carcinoma Transition Through PD-1/PD-L1 Checkpoint Remodeling

Parisa Kadkhodaei
Poursina Hakim Cancer Prevention Association
Samane Mohammadzadeh
Isfahan University of Medical Sciences
Safoora Mohammadzadeh
Isfahan University of Medical Sciences
Razieh Kamali
Islamic Azad University
Pouria Samadi
Isfahan University of Medical Sciences
Alireza Fahim
Isfahan University of Medical Sciences
Elham Amjadi
Isfahan University of Medical Sciences
Aida Heidari
University of Bologna
Mohammad Hassan Emami
Isfahan University of Medical Sciences
Fatemeh Maghool
f.maghool@pddrc.com

Isfahan University of Medical Sciences

Article

Keywords: Colorectal Cancer, advanced colorectal adenomas, PD-1, PD-L1, DNA Methylation, Immune Checkpoints, Tumor-Infiltrating Lymphocytes

Posted Date: September 1st, 2026

DOI: https://doi.org/10.21203/rs.3.rs-10593108/v1

License: This work is licensed under a Creative Commons Attribution 4.0 International License.
Read Full License

Additional Declarations: No competing interests reported.

Early Immune Dysregulation Emerges During the Advanced Adenoma–Carcinoma Transition Through PD-1/PD-L1 Checkpoint Remodeling

Author Names:

Parisa Kadkhodaei[1, 2*], Samane Mohammadzadeh[2, 3*], Safoora Mohammadzadeh[2, 3], Razieh Kamali[4, 5, 1], Pouria Samadi[2, 3], Alireza Fahim[2], Elham Amjadi[2], Aida Heidari[6], Mohammad Hassan Emami[2, 3**], Fatemeh Maghool[2, 3**].

[1]Poursina Hakim Cancer Prevention Association, Isfahan, Iran

[2]Poursina Hakim Digestive Diseases Research Center, Isfahan University of Medical Sciences, Isfahan, Iran

[3]Pooya Zist-Mabna Hakim Company, Poursina Hakim Institute, Isfahan, Iran

[4]Department of Medicine, Na.C., Islamic Azad University, Najafabad, Iran

[5]Clinical Research Development Center, Na.C., Islamic Azad University, Najafabad, Iran

[6]Department of Pharmacy and Biotechnology, University of Bologna, 40127 Bologna, Italy

*Parisa Kadkhodaei and Samane Mohammadzadeh contributed equally to this work and share first authorship.

** Mohammad Hassan Emami and Fatemeh Maghool share the corresponding author in this paper.

Corresponding author1: Poursina Hakim Digestive Diseases Research Center, Isfahan Healthcare City, Aghababaei Expy, Isfahan University of Medical Sciences, Isfahan, Iran; mh_emami@med.mui.ac.ir, ORCID: 0000-0001-5868-0182

Corresponding author2: Poursina Hakim Digestive Diseases Research Center, Isfahan Healthcare City, Aghababaei Expy, Isfahan University of Medical Sciences, Isfahan, Iran; f.maghool@gmail.com, f.maghool@pddrc.com, ORCID: 0000-0002-0845-4600

Abstract

Dysregulation of immune checkpoints, particularly PD-1 and PD-L1, drives colorectal cancer (CRC) progression. This case–control study investigated the stage- and sex-dependent transcriptional and epigenetic dynamics of *PDCD1* (PD-1) and *CD274* (PD-L1) across the normal–advanced adenoma (ACA)–CRC sequence, and evaluated their correlation with tumor-infiltrating lymphocytes (TILs). Quantitative RT-PCR and digestion-based promoter methylation assays (using *Hpa*II/*Msp*I) were performed on tissue specimens. We demonstrate a progressive transcriptional divergence: PD-1 expression significantly decreased from normal mucosa to ACA and CRC, whereas PD-L1 expression increased, peaking in CRC. This PD-L1 upregulation correlated with decreased exon methylation in ACA, indicating early epigenetic derepression. Notably, female ACA tissues exhibited significantly higher PD-L1 expression than male counterparts, highlighting early sex-specific immune modulation. Correlation analyses revealed progressive uncoupling of PD-1/PD-L1 expression and stage-specific shifts in methylation patterns. Furthermore, PD-1 methylation positively correlated with TIL density specifically in ACA, whereas lifestyle confounders showed no significant association. These findings reveal that PD-1 and PD-L1 undergo distinct transcriptional and epigenetic remodeling during early colorectal neoplasia. The identification of early sex-specific PD-L1 upregulation and altered expression-methylation coupling offers potential biomarkers and targets for early-stage immunotherapeutic intervention.

Keywords:

Colorectal Cancer; advanced colorectal adenomas, PD-1; PD-L1; DNA Methylation; Immune Checkpoints; Tumor-Infiltrating Lymphocytes

Background

Colorectal cancer (CRC) is the third most commonly diagnosed malignancy and the second leading cause of cancer-related mortality worldwide, accounting for approximately 935,173 deaths in 2020 according to GLOBOCAN estimates[1]. Epidemiological evidence indicates a concerning global increase in CRC incidence, including a rising trend of early-onset disease. In the United States, the incidence of colorectal adenocarcinoma among individuals aged 40–49 years increased by nearly 15% between 2000–2002 and 2014–2016. [2,3]. Comparable patterns have been observed across Asia and Western Asia, where both incidence and mortality rates continue to rise, with projections indicating a substantial escalation in disease burden by 2030 [4-6]. In Iran, CRC ranks as the fourth most common cancer in men and the second in women, with a marked increase in incidence over recent decades, likely reflecting demographic transitions and lifestyle modifications [7,8]. Established risk factors—including aging, family history, obesity, physical inactivity, smoking, and westernized dietary patterns—contribute significantly to this growing burden and impose considerable socioeconomic costs on healthcare systems worldwide [9-13].

At the molecular level, colorectal tumorigenesis is a multistep process driven by the progressive accumulation of genetic and epigenetic alterations, including mutations in key oncogenes and tumor suppressor genes such as Adenomatous Polyposis Coli (APC), KRAS, and Tumor Protein p53 (TP53) [14-16]. Among epigenetic mechanisms, aberrant DNA methylation plays a pivotal role in CRC pathogenesis by modulating gene expression and shaping tumor–immune interactions, thereby influencing immune checkpoint pathways critical for tumor immune evasion [17-20].

DNA methylation is one of the most extensively characterized epigenetic alterations implicated in CRC progression. Promoter hypermethylation can result in transcriptional silencing of tumor suppressor genes and dysregulation of immune-related pathways that govern tumor–host interactions [21,22]. Emerging evidence suggests that epigenetic modifications regulate the expression of immune checkpoint molecules, including Programmed Death-1 (PD-1) and Programmed Death-Ligand 1 (PD-L1), which are key mediators of immune tolerance within the tumor microenvironment [23-26]. Aberrant methylation within regulatory regions of these genes can alter transcriptional activity and consequently modulate anti-tumor immune responses. For example, hypermethylation of the PD-L1 promoter has been associated with reduced transcription

in certain tumor contexts, whereas hypomethylation of the PD-1 locus in chronically stimulated T cells may sustain receptor expression and contribute to T-cell exhaustion [26-29]. These findings underscore the central role of epigenetic remodeling in the regulation of immune checkpoint pathways during tumor development.

The PD-1/PD-L1 signaling axis constitutes a critical inhibitory pathway that regulates T-cell activation and immune homeostasis. PD-1 is primarily expressed on activated T lymphocytes, B cells, and natural killer cells, whereas PD-L1 is broadly expressed on tumor cells as well as antigen-presenting and stromal cells within the tumor microenvironment[29]. Engagement of PD-1 by PD-L1 initiates intracellular inhibitory signaling cascades that attenuate T-cell receptor (TCR) signaling, reduce cytokine production, and impair cytotoxic T-cell function [26,30,31]. Chronic antigenic stimulation within the tumor microenvironment promotes sustained PD-1 expression through transcriptional regulators such as nuclear factor of activated T cells (NFAT), ultimately leading to T-cell dysfunction and exhaustion [32,33]. Concurrently, PD-1/PD-L1 interactions activate downstream inhibitory pathways, including / Protein Phosphoinositide 3-Kinase / Kinase B (PI3K/AKT) and Rat Sarcoma Viral Oncogene (RAS) signaling, further suppressing effector T-cell responses and promoting regulatory T-cell expansion [34,35]. Collectively, these mechanisms contribute to the establishment of an immunosuppressive tumor microenvironment that facilitates tumor immune escape [36,37].

Although the clinical relevance of the PD-1/PD-L1 axis in established CRC has been extensively studied, considerably less is known about the dynamic epigenetic regulation of these immune checkpoints during the earliest stages of colorectal tumorigenesis. CRC typically develops through the well-characterized adenoma–carcinoma sequence, in which benign adenomatous lesions progressively accumulate molecular alterations that culminate in invasive carcinoma [38,39]. Advanced colorectal adenomas (ACAs), defined as adenomatous polyps ≥10 mm in size and/or those exhibiting villous histology or high-grade dysplasia, are recognized as high-risk precancerous lesions within this sequence. Owing to their substantial malignant potential, ACAs represent an optimal model for investigating early molecular and immunological alterations preceding invasive CRC. Increasing evidence indicates that immune dysregulation is initiated at the adenoma stage, well before clinical detection of invasive cancer [40,41]. However, the

epigenetic mechanisms governing immune checkpoint regulation during this transition remain insufficiently characterized.

Elucidating the epigenetic regulation of PD-1 and PD-L1 during the transition from advanced adenoma to carcinoma may provide critical insights into early immune escape and the establishment of an immunosuppressive microenvironment. Such insights may also facilitate the identification of epigenetic biomarkers for predicting disease progression and therapeutic responsiveness. Accordingly, in the present study, we investigated promoter methylation patterns of PD-1 and PD-L1 in patients with colorectal cancer and advanced colorectal adenomas, with the aim of characterizing the dynamic remodeling of immune checkpoint regulation during the adenoma–carcinoma transition and evaluating their potential as epigenetic biomarkers of early immune dysregulation, disease progression, and treatment response.

Results:

Demographic Data: The demographic characteristics of the study participants are summarized in Table 1. The proportion of males was higher in the CRC group (69.6 percent) and ACA group (62.5 percent) compared with the normal group (35.3 percent), while females were more prevalent in the normal group (64.7 percent). Despite these numerical differences, sex distribution did not differ significantly across the study groups ($P>0.05$), indicating no sex-related imbalance in this study.

Age distribution varied numerically across the study groups, with a higher proportion of participants aged ≥60 years in the ACA and CRC groups compared with the normal group, while younger individuals (<45 years) were more frequent in the normal group. However, these differences did not reach statistical significance ($P>0.05$), indicating no meaningful age-related imbalance among the groups. The mean age showed a significant upward trend across the groups (Normal: 57.12 ± 12.97 years; ACA: 59.58 ± 13.15 years; CRC: 66.52 ± 11.84 years; $P = 0.02$), data was not shown.

The distribution of body mass index (BMI) and smoking status among the study groups is shown in Table 1. Higher BMI values (>25 kg/m²) were more frequent in CRC patients (52.2%) compared with ACA (45.8%) and normal subjects (17.6%). Overweight individuals (BMI 25–30) were most

common in the normal group (52.9%). Similarly, the BMI was significantly lower in CRC patients compared with normal individuals (Normal: 28.27 ± 4.00; ACA: 26.91 ± 4.37; CRC: 25.05 ± 3.64; P = 0.01), data was not shown.

The distribution of smoking status did not differ significantly across the normal, ACA, and CRC groups (P > 0.05). Current smokers represented approximately one-third of participants in each group. Non-smokers were absent in the normal group but accounted for half of individuals in both the ACA and CRC groups. Former smokers were similarly distributed across groups.

The comparison of PD-1 and PD-L1 methylation and expression levels between normal tissues across the three groups (normal, ACA, and CRC) and between diseased and adjacent normal tissues in ACA and CRC revealed statistically significant differences only in the cases indicated in Figure 1.

Enzymatic methylation of PD-1 (H, M, and total forms) showed no statistically significant differences among the three groups and also between diseased tissues and adjacent tissues in ACA and CRC groups, Figure 1A. A marked decrease in PD-1 expression (PD-1. Exp. N) was observed from normal tissue to ACA and CRC (PD-1 expression vs. normal: 1.07 ± 0.39 vs. 0.73 ± 0.21 vs. 0.59 ± 0.27; P = 0.006), Figure 1A and 1B. A similar trend was found when comparing PD-1 expression (PD-1.exp.Adj) to adjacent normal tissue (P = 0.007). PD-1 expression (PD-1. Exp. N) was significantly reduced in ACA tissue compared to normal adjacent ACA tissue (Normal adjacent ACA: 1.00 ± 0.18; ACA: 0.73 ± 0.21; P = 0.004) and CRC tissue compared to normal adjacent CRC (Normal adjacent CRC: 1.07 ± 0.39; CRC: 0.59 ± 0.27; P = 0.009).

The level of PD-L1 exon methylation by HpaII restriction enzyme (PD-L1. Meth.H) was significantly reduced in CRC compared to normal and ACA tissues (Normal: 206.84 ± 123.44; ACA: 94.49 ± 67.11; CRC: 15.49 ± 6.44; P = 0.04). The methylation level of the PD-L1 exon, assessed using the MspI restriction enzyme (PD-L1. Meth.M), was lower in CRC tissues compared with normal and ACA tissues; however, these differences did not reach statistical significance. A

consistent reduction was also found for total PD-L1methylation (PD-L1. Meth. Total), (Normal: 244.14 ± 152.50; ACA: 104.25 ± 102.18; CRC: 15.73 ± 4.13; P = 0.05). The level of PD-L1 exon methylation, HpaII restriction enzyme and PD-L1 total methylaton (PD-L1. Meth.H and PD-L1. Meth.Total) were significantly reduced in ACA compared to normal adjacent ACA tissues (P = 0.034 and P = 0.018). The methylation level of the PD-L1 exon, assessed using the MspI restriction enzyme (PD-L1. Meth.M), was lower in ACA tissues compared with normal adjacent ACA tissues, however, these differences did not reach statistical significance. A consistent reduction was also found for total PD-L1 methylation (PD-L1. Meth. Total) in CRC group, however, differences were not significant.

In contrast, PD-L1 gene expression (PD-L1. Exp. N) was significantly upregulated in CRC compared to normal and ACA tissues (PD-L1 expression vs. normal: 1.03 ± 0.25, 0.86 ± 0.28, and 1.27 ± 0.30, respectively; P = 0.003). Notably, when compared to adjacent normal tissue, PD-L1 expression (PD-L1. Exp. Adj) increased markedly across the progression from ACA to CRC (Normal: 1.03 ± 0.25; ACA: 1.37 ± 0.45; CRC: 7.57 ± 1.80; P < 0.0001). For PD-L1 expression, PD-L1. Exp. N was significantly elevated in CRC (P=0.014) compared to normal adjacent CRC tissue and, PD-L1. Exp. Adj was significantly elevated in ACA (P=0.036) and CRC (P=0.000) tissues compared their normal adjacent tissues, Figure 1C and 1D.

No significant differences were observed in PD-1, PD-L1 methylation and expression levels between normal tissue with adjacent normal tissues in ACA and CRC and the values were generally similar across the groups.

In addition, although TILs were more abundant in CRC tissues than in ACA tissues, this difference did not reach statistical significance, data was not shown.

The analysis of PD-1 and PD-L1 expression and methylation between males and females in normal individuals, ACA, and CRC patients showed statistically significant differences only for PD-L1 expression, Table 2. In normal tissue, ACA and tumor tissues, PD-1 methylations in Male were higher than Females, but they were not significant. In different tissues, PD-L1 methylations in Male and Females were similar. In Normal tissue and tumor tissues, PD-1 expression in Females were higher than Male, but they were not significant and in ACA tissues PD-1 expression in Male and Females were similar. In normal and CRC tissues, PD-L1 expression were slightly higher in females than males, however were not significant. In ACA, PD-L1 expression was significantly higher in females than males (Females: 1.09 ± 0.03 vs. Males: 0.80 ± 0.29 and Females: 1.74 ± 0.04 vs. Males: 1.28 ± 0.46, respectively in PD-L1Expression versus Normal tissue (PD-L1. Exp. N) and PD-L1expression versus Adjacent Normal tissue (PD-L1. Exp. Adj) ($P = 0.01$).

The expression and methylation levels of PD-1 and PD-L1 in normal tissue, ACA tissue, and tumor tissue did not show significant differences with respect to age groups, body mass index, or TIL categories. The data were not shown.

Correlation Between PD-1 and PD-L1 Expression

The relationship between PD-1 and PD-L1 expression was assessed in normal tissue, ACA tissue, tumor tissue, adjacent normal tissues of ACA and CRC, Table 3. In normal tissue, PD-1 expression versus Normal (PD-1.exp.N) and PD-1.exp.Adj (PD-1.exp.Adj) showed a strong positive correlation with PD-L1 expression versus Normal (PD-L1.exp.N) and also PD-L1 expression versus Adj.Normal (PD-1.exp.Adj) (Pearson's r = 0.750, P = 0.013, n = 10), indicating a significant association. In ACA tissue, the correlation between PD-1 and PD-L1 expression was moderate but not statistically significant (Pearson's r = 0.419, P = 0.228, n = 10). In adjacent normal tissues of ACA, the correlation between PD-1 and PD-L1 expression was weakly (Pearson's r = -0.116, P = 0.734, n = 11). In tumor tissue, PD-1 and PD-L1 expression were weakly correlated and the association was not significant (Pearson's r = 0.072, P = 0.843, n = 10). In adjacent normal tissues of CRC, the correlation between PD-1 and PD-L1 expression was moderate but not statistically significant (Pearson's r = -0.556, P = 0.120, n = 9).

The correlation analysis between PD-1 and PD-L1 (PD-L1) methylation levels across five tissue types revealed distinct patterns of association, Table 4.

In Normal tissue, a strong and statistically significant negative correlation was observed between PD-1. Meth.H and PD-L1. Meth.H (r = –0.832, p = 0.010), as well as between PD-1. Meth.Total and PD-L1. Meth.H (r = –0.844, p = 0.008). No significant correlations were found for methylation in the M region or total methylation of PD-L1 with other PD-1 parameters. These findings suggest an inverse relationship between PD-1 and PD-L1 methylation patterns in this tissue type.

In ACA tissue, no significant correlations were detected between PD-1 and PD-L1 methylation levels in any region (H, M, or Total), indicating independent methylation behavior of these genes in this tissue.

In CRC tissue, a significant positive correlation was observed between PD-1. Meth.M and PD-L1. Meth.Total (r = 0.766, p = 0.027), whereas no significant associations were seen for other regions. This suggests that methylation of the M region of PD-1 may be linked to overall PD-L1 methylation in this tissue.

In Adjacent normal tissues of ACA, multiple significant positive correlations were identified. PD-1. Meth.M was strongly correlated with both PD-L1. Meth.M ($r = 0.734$, $p = 0.004$) and PD-L1. Meth.Total ($r = 0.656$, $p = 0.015$). Additionally, PD-1. Meth.Total was positively associated with PD-L1. Meth.M ($r = 0.626$, $p = 0.022$) and PD-L1. Meth.Total ($r = 0.570$, $p = 0.042$). These findings indicate coordinated methylation regulation between PD-1 and PD-L1 in this tissue type.

In Adjacent normal tissues of CRC, positive but non-significant correlations were found between all PD-1 and PD-L1 methylation regions (r range: 0.395–0.543, $p > 0.16$), suggesting a trend toward co-methylation without statistical significance.

The correlation analysis between gene expression and methylation levels of PD-1 and PD-L1 (PD-L1) across five tissue types revealed variable tissue-dependent relationships, Supplementary Table 1.

In Normal tissue, PD-1 expression showed a strong positive correlation with PD-1. Meth.H ($r = 0.895$, $p = 0.105$) but did not reach statistical significance, while no meaningful associations were observed for the M or Total methylation regions. Similarly, PD-L1 expression demonstrated a negative but non-significant correlation with PD-L1. Meth.H ($r = –0.807$, $p = 0.193$). These data indicate a potential inverse trend between expression and promoter methylation of PD-L1 in this tissue, albeit without statistical significance.

In ACA tissue, no significant correlations were detected between the expression levels of either PD-1 or PD-L1 and their respective methylation status in any analyzed region (H, M, or Total), suggesting no apparent epigenetic–transcriptional linkage in this tissue.

In CRC tissue, PD-1 expression displayed a moderate positive correlation with PD-1. Meth.M ($r = 0.472$, $p = 0.285$), whereas PD-L1 expression exhibited a strong positive, though non-significant, correlation with PD-L1. Meth.M ($r = 0.856$, $p = 0.064$). This suggests that methylation in the M region may have a regulatory relationship with gene expression in this tissue type.

In Adjacent normal tissues of ACA, PD-1 expression was strongly and significantly correlated with both PD-1. Meth.M ($r = 0.969$, $p = 0.001$) and PD-1. Meth. Total ($r = 0.844$, $p = 0.035$). No

significant associations were detected between PD-L1 expression and methylation patterns, though all correlations were negative, indicating an inverse trend.

In Adjacent normal tissues of CRC, PD-1 expression exhibited significant positive correlations with PD-1. Meth.H ($r = 0.868$, $p = 0.011$) and PD-1. Meth. Total ($r = 0.804$, $p = 0.029$). In contrast, PD-L1 expression showed consistently negative but non-significant correlations across all methylation regions ($r \approx –0.43$, $p > 0.46$).

The correlation analysis between gene methylation/expression levels of PD-1 and PD-L1 (PD-L1) and the degree of TILs in ACA tissues revealed selective and gene-specific associations.

A significant positive correlation was observed between PD-1. Meth.H and TIL density ($r = 0.586$, $p = 0.036$), suggesting that higher methylation in the H region of PD-1 may be associated with increased lymphocytic infiltration in ACA. Moderate, but non-significant, positive correlations were also noted between PD-1. Meth.M ($r = 0.417$, $p = 0.156$) and PD-1. Meth.Total ($r = 0.482$, $p = 0.095$) with TILs. In contrast, PD-1 expression levels (both relative to normal and adjacent normal tissues) showed no significant association with TIL density ($r = –0.062$, $p = 0.866$), supplementary Table 2.

For PD-L1 (PD-L1), all correlations between methylation or expression levels and TILs were negative but statistically non-significant, including PD-L1. Meth.H ($r = –0.322$, $p = 0.143$), PD-L1. Meth.M ($r = –0.157$, $p = 0.486$), and PD-L1. Meth.Total ($r = –0.210$, $p = 0.349$). Similarly, PD-L1 expression relative to both normal and adjacent normal tissues was not significantly correlated with TILs ($r = –0.209$, $p = 0.562$), Supplementary Table 2.

Discussion

This study demonstrated a progressive reprogramming of immune checkpoint regulation along the normal mucosa–ACA– CRC continuum, characterized by reduced PD-1 expression and increased PD-L1 expression during colorectal tumorigenesis. PD-1 expression declined significantly from normal mucosa to ACA and CRC, whereas PD-L1 expression increased, particularly in CRC and in diseased tissues relative to their adjacent normal counterparts. Epigenetically, PD-L1 methylation assessed by HpaII digestion was significantly reduced in CRC, and exon-specific as well as total PD-L1 methylation also showed a downward trend, with significant reductions in ACA compared with adjacent normal tissues. In contrast, PD-1 methylation remained largely stable across tissue groups. TIL density appeared higher in CRC than in ACA, although this difference did not reach statistical significance.

The demographic and lifestyle characteristics of the study population were broadly consistent with established epidemiological patterns of colorectal neoplasia. Although males were numerically more frequent in the ACA and CRC groups, sex distribution did not differ significantly between groups, suggesting that sex was unlikely to confound the molecular and epigenetic findings. Aging is accompanied by cumulative molecular and cellular alterations, including genomic instability, chronic low-grade inflammation, immune senescence, and epigenetic drift, all of which contribute to increased susceptibility to malignant transformation. In particular, age-associated DNA methylation changes progressively accumulate during colorectal carcinogenesis and may influence the expression of genes involved in immune regulation, inflammation, and tumor suppression. Such epigenetic alterations are considered early events in the adenoma–carcinoma transition and may facilitate the establishment of a pro-tumorigenic microenvironment. Therefore, the higher age observed in ACA and CRC patients may reflect not only prolonged exposure to environmental and endogenous risk factors but also the cumulative burden of age-related epigenetic and immunological changes that drive colorectal cancer progression. [41-43]. By contrast, BMI followed a stage-dependent pattern, with CRC patients exhibiting significantly lower BMI than the normal and ACA groups, consistent with tumor-associated metabolic dysregulation and cancer-related cachexia in advanced disease. This finding is in agreement with the well-established concept that progression to colorectal cancer is accompanied by profound metabolic alterations and the development of cancer-associated cachexia. Cancer cachexia is a multifactorial syndrome

characterized by systemic inflammation, increased energy expenditure, enhanced proteolysis and lipolysis, and progressive loss of skeletal muscle and adipose tissue, ultimately leading to involuntary weight loss and reduced BMI. In colorectal cancer, pro-inflammatory mediators such as interleukin 1 beta (IL-1β), IL-6, and TNF-α contribute to metabolic dysregulation and tissue wasting, particularly in advanced disease stages. Therefore, the lower BMI observed in CRC patients may reflect the cumulative effects of tumor burden and cachexia-related metabolic disturbances. These findings are consistent with previous evidence demonstrating that low BMI and body weight loss are common manifestations of colorectal cancer progression and are associated with unfavorable clinical outcomes and impaired nutritional status [44,45]. Smoking status did not differ significantly across groups, indicating a limited likely contribution to the molecular patterns observed in this cohort .Therefore, the differences identified are more likely attributable to disease-related biological processes rather than confounding effects of smoking, despite the well-established role of cigarette smoking as a recognized risk factor for colorectal neoplasia.

At the molecular level, the progressive reduction in PD-1 expression across the normal–ACA–CRC sequence likely reflects dynamic changes in immune cell composition and T-cell functional states within the evolving tumor microenvironment rather than direct transcriptional silencing alone. PD-1 is predominantly expressed on activated and chronically stimulated T lymphocytes, where it exerts inhibitory effects through Src Homology 2 Domain-Containing Protein Tyrosine Phosphatase 2 (SHP-2) -mediated attenuation of TCR and Cluster of Differentiation28 (CD28) signaling. Persistent antigenic stimulation within neoplastic tissues promotes T-cell exhaustion and reshapes PD-1-associated signaling networks, ultimately leading to impaired effector function and immune dysfunction. Moreover, progression from adenoma to carcinoma is accompanied by substantial remodeling of the tumor microenvironment, including altered immune cell infiltration and enrichment of immunosuppressive populations, which may further contribute to the observed decline in PD-1 expression [46-48]. Therefore, reduced PD-1 expression in tumor tissues may indicate shifts in lymphocyte subsets, immune exclusion, or spatial heterogeneity of infiltrating immune cells. This interpretation is consistent with prior CRC studies showing that PD-1 expression is strongly influenced by immune localization and tumor microenvironmental context [32,49].

In contrast, PD-L1 expression increased toward CRC and was accompanied by reduced exon and total methylation, particularly in ACA tissues. PD-L1 is a transmembrane ligand that suppresses T-cell activation through interaction with PD-1 ,thereby supporting immune tolerance within the tumor microenvironment. Its transcription is controlled by inflammatory signaling pathways, including Interferon Gamma/ Janus Kinase- Signal Transducer and Activator of Transcription (IFN-γ/JAK–STAT), Nuclear Factor Kappa B (NF-κB), and oncogenic Phosphoinositide 3-Kinase- Protein Kinase B- Mechanistic Target of Rapamycin (PI3K–AKT–mTOR) and Mitogen-Activated Protein Kinase (MAPK) cascades [39,50]. Hypomethylation of PD-L1 regulatory regions can increase chromatin accessibility and facilitate transcription, thereby enhancing PD-L1 expression in malignancy. The inverse relationship observed here between PD-L1 methylation and expression is therefore biologically plausible and aligns with previous CRC evidence showing that promoter methylation of PD-L1 is inversely associated with transcript abundance and may have prognostic relevance [23,24,51]. The more pronounced methylation shifts in ACA than CRC may indicate that epigenetic deregulation begins early during neoplastic transformation and later becomes more heterogeneous as additional genetic and microenvironmental changes accumulate. At the same time, locus-specific and method-dependent differences reported in the literature suggest that PD-L1 methylation patterns may vary substantially across cohorts and CpG regions analyzed [14,28,52]. The lack of significant differences in PD-1 methylation across tissue groups suggests that PD-1 downregulation is unlikely to be explained primarily by stable promoter methylation changes in this cohort. Instead, transcriptional regulation, immune-cell composition, and microenvironmental context may play stronger roles. This finding is consistent with evidence that PD-1 expression in CRC is highly context dependent and often reflects the abundance and functional state of immune infiltrates rather than a uniform epigenetic program.

Sex-specific analyses revealed a significant difference only in PD-L1 expression, which was higher in females than in males in ACA tissues, whereas PD-1 expression and methylation levels of both genes did not differ significantly between sexes. This may reflect sex-dependent immune regulation during early colorectal neoplasia. Experimental studies suggest that estrogen signaling can modulate immune checkpoint pathways through estrogen receptor–mediated transcriptional effects and interferon-related cascades, potentially influencing PD-L1 induction[53-55]. In this

context, elevated PD-L1 expression in females at the ACA stage may represent an immune-adaptive response rather than a definitive marker of immune escape.

Correlation analyses further revealed tissue-specific regulatory dynamics across the normal–ACA–CRC continuum, highlighting progressive disruption of immune checkpoint homeostasis during colorectal tumorigenesis. The strong positive correlation between PD-1 and PD-L1 expression observed in normal mucosa suggests coordinated regulation of the PD-1/PD-L1 axis under physiological conditions, which is essential for maintaining mucosal immune tolerance and preventing excessive inflammatory responses in the intestine. The gradual attenuation of this relationship in ACA and CRC tissues may reflect increasing immune dysregulation and remodeling of the tumor microenvironment, accompanied by changes in the abundance and functional states of infiltrating immune cells. In parallel, the transition from inverse methylation correlations in normal tissues to independent patterns in ACA and emerging positive associations in CRC indicates progressive epigenetic reprogramming during neoplastic evolution. Such changes are consistent with the concepts of field cancerization and methylation instability, whereby widespread alterations in DNA methylation patterns accumulate throughout colorectal carcinogenesis and contribute to the establishment of a permissive tumor microenvironment. Moreover, increasing concordance between PD-1 and PD-L1 methylation in CRC may suggest the emergence of common epigenetic regulatory mechanisms driven by chronic inflammation, genomic instability, and aberrant DNA methyltransferase activity. Collectively, these findings support the notion that disruption of coordinated checkpoint regulation and epigenetic remodeling are integral components of the adenoma–carcinoma sequence and may contribute to immune escape during colorectal cancer progression. [21,42,56-59].

Finally, In ACA tissues, the observed significant positive association between PD-1 promoter methylation in the H region and tumor-infiltrating lymphocyte (TIL) density suggests that epigenetic modulation of PDCD1 may partially mirror early immune microenvironment dynamics during neoplastic transformation. This relationship may reflect a context-dependent interplay between immune cell infiltration and epigenetic remodeling, in which local inflammatory cues and T-cell–derived signals influence DNA methylation patterns in surrounding stromal and immune cells. Notably, PD-1 expression levels and PD-L1-related variables did not demonstrate a significant correlation with TIL density, indicating that transcriptional output of the PD-1 axis is not solely determined by the extent of lymphocytic infiltration in early

adenomatous lesions. In contrast, the lack of a direct association between PD-L1 expression and TIL abundance suggests that PD-L1 regulation is governed by a more complex network of tumor-intrinsic and extrinsic factors, including interferon-γ–driven inflammatory signaling, oncogenic pathway activation (such as PI3K/AKT and MAPK), and stromal–epithelial crosstalk within the tumor microenvironment. These mechanisms may decouple PD-L1 expression from simple immune cell density, reflecting adaptive immune resistance rather than passive immune presence [31,60]. Collectively, these findings support a model in which PD-1 epigenetic alterations may serve as a sensitive, early indicator of immune–epigenetic interaction during adenoma progression, whereas PD-L1 expression is predominantly shaped by integrated inflammatory and tumor-intrinsic signaling networks rather than TIL quantity alone.

This case–control study delineates the dynamic modulation of PD-1 and PD-L1 expression and methylation along the normal–ACA–CRC continuum, highlighting stage- and sex-specific immune regulatory patterns. PD-1 expression progressively declined from normal mucosa to ACA and CRC, whereas PD-L1 expression increased, particularly in CRC tissues, accompanied by partial epigenetic derepression. Notably, elevated PD-L1 expression in female ACA suggests early sex-dependent immune checkpoint modulation. The observed decoupling of PD-1 and PD-L1 expression and shifts in methylation correlations underscore the context-dependent regulation of immune checkpoints, potentially reflecting early immune dysregulation and adaptive responses within the tumor microenvironment. Collectively, these findings provide mechanistic insights into local immune modulation in colorectal tumorigenesis and underscore the importance of considering demographic and molecular factors in interpreting immune checkpoint biology.

Methods

A case–control study was conducted between 2019 and 2022 at the Poursina Hakim Gastrointestinal Clinic in Isfahan, Iran, enrolling patients diagnosed with CRC or ACA, along with age-matched healthy controls (30–75 years). The study protocol was approved by the Ethics Committee of Isfahan University of Medical Sciences (IR.ARI.MUI.REC.1401.337), and written informed consent was obtained from all participants prior to enrollment. All methods were performed in accordance with the relevant institutional, national, and international guidelines and regulations. All colonoscopic procedures were performed by experienced gastroenterologists.

Group allocation (CRC, ACA, or healthy control) was determined based on histopathological evaluation of biopsy or resection specimens. Inclusion criteria comprised individuals aged 20–85 years who were referred for CRC screening or presented with gastrointestinal symptoms, including melena, hematochezia, positive fecal occult blood test, anemia, or dyspepsia. Exclusion criteria were refusal to participate, prior history of adenomatous polyps or malignancy, hereditary colorectal cancer syndromes (e.g., Lynch syndrome), pregnancy, inflammatory bowel disease, or previous chemotherapy and/or radiotherapy. ACA were defined according to established pathological criteria as lesions exhibiting at least one of the following features: size >10 mm, villous or tubulovillous histology, or high-grade dysplasia. All participants completed a structured questionnaire capturing demographic characteristics, family history of CRC, use of dietary supplements, and aspirin consumption.

Sample Collection and DNA Extraction

Two tissue biopsies were collected from each participant: one from the primary tumor or adenomatous lesion, and another from the adjacent normal mucosa for comparative analysis, in both CRC and ACA patients. Additionally, normal colorectal tissue specimens were obtained from healthy control subjects. Genomic DNA was isolated from all biopsy samples utilizing the DNA Extraction Kit (ADDBIO, Daejeon, Korea) according to the manufacturer's protocol. DNA concentration and purity were assessed via Nano Drop spectrophotometry (Maestrogen, Taiwan), and DNA integrity was examined through agarose gel electrophoresis.

DNA Methylation Analysis

Assessment of CpG Methylation by Methylation-Sensitive Restriction Enzyme (MSRE)-qPCR

The DNA methylation status of CpG sites within the regulatory regions of PD-1 and PD-L1 was determined using a MSRE-qPCR approach. This method exploits the differential methylation sensitivity of the isoschizomers Thermo Fisher Scientific HpaII and MspI, which recognize the same CCGG sequence but display distinct cleavage patterns depending on cytosine methylation status. Under unmethylated conditions, both enzymes efficiently cleave the CCGG site. However, their activities diverge when cytosine methylation is present. MspI cleaves the site when the internal cytosine is methylated on one or both strands, provided the external cytosine remains

unmethylated, rendering it insensitive to internal CpG methylation but inhibited by methylation of the outer cytosine. In contrast, HpaII cleaves only fully unmethylated sites or hemimethylated configurations at the external cytosine and is inhibited by symmetrical methylation. The complementary sensitivities of these enzymes enable discrimination among unmethylated, hemimethylated, and fully methylated CpG configurations. Accordingly, differences in Polymerase Chain Reaction (PCR) amplification following HpaII digestion reflect relative methylation levels at the PD-1 and PD-L1 loci across CRC, ACA, and normal tissue samples.

Methylation-Specific Restriction Digestion

For each DNA sample, parallel digestion reactions were prepared using equal amounts of normalized genomic DNA. Three reaction conditions were included: (i) mock digestion without enzyme (sham control), (ii) digestion with a methylation-sensitive restriction enzyme (HpaII or MspI), and (iii) an enzymatic control to verify digestion efficiency. Each sample (5 µL; 1–300 ng/µL) was incubated overnight at 37 °C in a final volume of 10 µL containing 1× Tango™ buffer (Fermentas) and 5 U of either HpaII or MspI. Enzymes were subsequently heat-inactivated at 70 °C for 20 min, and digested DNA was stored at 4 °C until quantitative analysis.

Primer Design and Quantitative Real-Time PCR

Primer pairs were designed to amplify genomic regions flanking informative MSRE recognition sites, ensuring that all CCGG sites were located within the amplicon boundaries but outside primer annealing regions. Primer design was performed using Primer3 and evaluated with Oligo7 according to established qPCR criteria outlined in the QuantiTect™ SYBR® Green PCR Handbook (Qiagen). Amplicon lengths were restricted to 100–200 bp to optimize amplification efficiency. Genomic reference sequences were retrieved from the UCSC Genome Browser (version mm6). All primer sets were empirically validated for optimal annealing temperature and specificity, Table 5.

Quantitative real-time PCR was performed using a Rotor-Gene 6000 system (Corbett Research). Reactions were carried out in duplicate using RealQ Plus 2× Master Mix Green High ROX (Thermo Fisher Scientific) in a total volume of 10 µL containing 1 µL of digested DNA, 0.5 µM of each primer, and 5 µL of 2× master mix. Cycling conditions consisted of an initial denaturation

at 95 °C for 15 min, followed by 45 cycles of 95 °C for 10 s, 60 °C for 15 s, and 72 °C for 10 s. Melting curve analysis (50–95 °C; ramp rate 0.2 °C/s) was performed to confirm product specificity. Digested non-methylated blood DNA was included in each run as a 0% methylation control.

Quantification of Promoter Methylation

Promoter methylation levels were calculated based on Delta Cycle Threshold (ΔCt) values derived from MSRE-qPCR data. Percentage methylation (%Me) was determined using the equation:

$$\%\boldsymbol{Methylation} = \mathbf{100} \times \boldsymbol{e}^{-\mathbf{0.7}(\boldsymbol{\Delta Ct})}$$

where ΔCt represents the difference between the Ct value of the digested sample and the corresponding reference control. To enhance analytical robustness and minimize bias related to reference selection, ΔCt values were calculated using two independent normalization strategies: External normalization against colorectal tissue obtained from healthy individuals, providing a physiological baseline for promoter methylation. Internal normalization against matched adjacent normal tissue from the same patient, controlling for inter-individual variability and local epigenetic field effects. Accordingly, two methylation values were generated for each gene in every study group: (i) methylation relative to healthy control tissue, and (ii) methylation relative to matched adjacent normal tissue. This dual-normalization framework enables discrimination between systemic disease-associated epigenetic alterations and tumor-specific promoter remodeling within the local microenvironment. Normalization to healthy controls facilitates baseline comparison, whereas normalization to adjacent tissue isolates tumor-driven epigenetic changes while accounting for patient-specific variability. Collectively, this strategy improves the biological interpretability and reliability of promoter methylation measurements in CRC and ACA specimens.

RNA Isolation and Quantitative Gene Expression Analysis

Total RNA was isolated using Trizol reagent (mXcell, Carlsbad, CA, USA) according to the manufacturer's instructions. RNA concentration and purity were determined spectrophotometrically using a NanoDrop instrument (Maestrogen, Taiwan), and only samples meeting established quality criteria were used for downstream analyses. Complementary DNA

(cDNA) was synthesized from purified RNA using the First-Strand Complementary DNA (cDNA) Synthesis Kit (Sinaclon, Tehran, Iran).

Primers were designed using Primer3 and subsequently validated in silico with Oligo7 to ensure specificity, optimal melting temperature, and absence of secondary structures, Table 6.

Quantitative real-time PCR (qRT-PCR) was performed using RealQ Plus 2× Master Mix Green High ROX (Thermo Fisher Scientific, Waltham, MA, USA). Each 10 µL reaction contained 1 µL cDNA template, 2 pM of each gene-specific primer, and 5 µL of 2× Master Mix. Amplification was conducted with an initial denaturation step at 95 °C for 10 min, followed by 40 cycles of denaturation at 95 °C and gene-specific annealing/extension conditions. For PD-1, cycling parameters were 95 °C for 30 s, 60 °C for 30 s, and 72 °C for 30 s. For PD-L1, amplification was performed at 95 °C for 15 s, 62 °C for 1 min, and 72 °C for 30 s, followed by a final extension at 72 °C for 1 min. Primer sequences are provided in Table 2. Relative gene expression levels of PD-1 and PD-L1 were calculated using the $2^{-}\Delta\Delta Ct$ method, with Actin Beta (ACTB) serving as the endogenous reference gene. To enhance the robustness and biological interpretability of transcriptional analyses, relative expression values were calculated using two independent biological comparators. First, gene expression was normalized to colorectal tissue obtained from healthy individuals, representing an external physiological baseline. Second, expression levels were independently normalized to matched adjacent normal tissue from the same patient, serving as an internal control to account for inter-individual variability and local tissue-specific influences. This dual-normalization strategy enabled comprehensive evaluation of immune checkpoint gene regulation by distinguishing systemic disease-associated alterations from tumor-specific transcriptional changes within the local microenvironment.

Tumor infiltration lymphocytes assessment:

TILs were evaluated on hematoxylin and eosin (H&E)-stained sections according to international consensus guidelines for TIL assessment. For each case, a single representative slide was selected, and the predominant spatial distribution pattern of TILs was documented. Stromal TILs (sTILs) were assessed at the invasive margin and quantified as the percentage of intratumoral stromal area occupied by mononuclear inflammatory cells relative to the total stromal area. Areas of necrosis,

hemorrhage, tissue artifacts, biopsy-related changes, and regions outside the tumor borders were excluded from analysis. Intratumoral TILs and lymphocytes associated with non-invasive components were not considered. Evaluation was performed in five representative high-power fields (×400 magnification), and the mean percentage across fields was calculated to account for intratumoral heterogeneity. In cases demonstrating heterogeneous lymphocytic distribution, the average density across the entire assessed area was recorded rather than focusing on hotspot regions. TIL percentages were rounded to the nearest 5% for reporting. For statistical analyses, sTILs were initially treated as a continuous variable and subsequently categorized into three predefined groups: <10%, 10–40%, and >40%.

Statistical Analysis

All statistical analyses were performed using R software (version 4.5.1). Descriptive statistics were used to summarize participant characteristics. Continuous variables were reported as mean ± standard deviation (SD). Categorical variables were presented as frequency (percentage). Normality of data distribution was assessed using the Shapiro–Wilk test. Comparisons of demographic characteristics (e.g., sex, smoking status) among the CRC, ACA, and control groups were conducted using the Chi-square test. Comparisons of PD-1 and PD-L1 methylation and gene expression levels among CRC, ACA, and control tissues were performed using the Kruskal–Wallis test. When significant differences were detected in non-parametric analyses, Dunn's post hoc test with multiple comparison adjustment was applied. To evaluate differences in methylation and expression levels among normal tissues of the three groups (healthy controls, ACA-adjacent normal tissues, and CRC-adjacent normal tissues), Kruskal–Wallis tests were used according to distributional assumptions. Comparisons between diseased tissues and their corresponding adjacent normal tissues within the ACA and CRC groups were conducted using Wilcoxon signed-rank tests. Demographic-based comparisons of PD-1 and PD-L1 methylation and expression levels within healthy controls, ACA patients, and CRC patients were performed using Mann–Whitney U tests. Pearson correlation analysis was used to evaluate associations between PD-1 and PD-L1 expression levels, as well as between their methylation levels, in normal, ACA, CRC, and adjacent normal tissues. Expression–methylation coupling was assessed using Pearson correlation coefficients between gene expression and corresponding methylation levels for PD-1 and PD-L1 across all tissue categories. Additionally, correlations between PD-1 and PD-L1 methylation and

expression levels and TIL density in five groups were examined using Pearson correlation analysis. When normality assumptions were not satisfied, Spearman's rank correlation test was applied. All tests were two-sided, and a p-value < 0.05 was considered statistically significant.

Reference

1 Bray, F. *et al.* Global cancer statistics 2022: GLOBOCAN estimates of incidence and mortality worldwide for 36 cancers in 185 countries. *CA: a cancer journal for clinicians* **74**, 229-263 (2024).

2 Siegel, R. L. *et al.* Global patterns and trends in colorectal cancer incidence in young adults. *Gut* **68**, 2179-2185 (2019).

3 Sung, H. *et al.* Colorectal cancer incidence trends in younger versus older adults: an analysis of population-based cancer registry data. *The Lancet Oncology* **26**, 51-63 (2025).

4 Rahimi, F. *et al.* Incidence of colorectal cancer in Iran: A systematic review and meta-analysis. *Journal of Research in Medical Sciences* **29**, 65 (2024).

5 Deng, Y. *et al.* Global, regional, and national disease burden and prediction analysis of colorectal cancer attributable to tobacco, alcohol, and obesity from 1990 to 2030. *Frontiers in Oncology* **15**, 1524308 (2025).

6 Arnold, M. *et al.* Global patterns and trends in colorectal cancer incidence and mortality. *Gut* **66**, 683-691 (2017).

7 Rafiemanesh, H. *et al.* Incidence and mortality of colorectal cancer and relationships with the human development index across the world. *Asian Pacific Journal of Cancer Prevention* **17**, 2465-2473 (2016).

8 Rafiemanesh, H. *et al.* Colorectal cancer in Iran: Epidemiology and morphology trends. *EXCLI journal* **15**, 738 (2016).

9 Keum, N. & Giovannucci, E. Global burden of colorectal cancer: emerging trends, risk factors and prevention strategies. *Nature reviews Gastroenterology & hepatology* **16**, 713-732 (2019).

10 Emami, M. H. *et al.* A review of heavy metals accumulation in red meat and meat products in the Middle East. *Journal of Food Protection* **86**, 100048 (2023).

11 Emami, M. H. *et al.* A Brief Meta-analysis and Health Risk Assessment of Lead and Cadmium in Meat, Liver, and Kidney of Livestock in Iran. *Current Nutrition & Food Science* **20**, 1126-1137 (2024).

12 Maghool, F. *et al.* Rescue effect of curcumin against copper toxicity. *Journal of Trace Elements in Medicine and Biology* **78**, 127153 (2023).

13 Emami, M. H. *et al.* Calcium and dairy products in the chemoprevention of colorectal adenomas: a systematic review and meta-analysis. *Critical reviews in food science and nutrition* **62**, 7168-7183 (2022).

14 Zoratto, F. *et al.* Focus on genetic and epigenetic events of colorectal cancer pathogenesis: implications for molecular diagnosis. *Tumor Biology* **35**, 6195-6206 (2014).

15 Zaurito, A. E. *An extensive cellular and molecular chart of genetic models elucidating the onset and progression of colorectal cancer*, Technische Universität München, (2025).
16 Chen, Y., Zhang, J., Ding, Y., Zhu, F. & Chen, Y. Colorectal cancer pathogenesis, oncogenic signaling networks and targeted therapeutic advances. *Molecular biomedicine* **7**, 32 (2026).
17 Issa, J.-P. Aging and epigenetic drift: a vicious cycle. *The Journal of clinical investigation* **124**, 24-29 (2014).
18 Baylin, S. B. & Jones, P. A. Epigenetic determinants of cancer. *Cold Spring Harbor perspectives in biology* **8**, a019505 (2016).
19 Maghool, F. *et al.* The immunoregulatory role of lncRNA UCA1: a pan-cancer perspective with a focus on colorectal cancer. *Naunyn-Schmiedeberg's Archives of Pharmacology* **399**, 3843-3862 (2026).
20 Maghool, F. *et al.* Exploring SLC30A6 as a potential prognostic, immunomodulatory, and therapeutic biomarker in various cancers with a focus on pancreatic cancer: a pan-cancer analysis. *Egyptian Journal of Medical Human Genetics* **25**, 138 (2024).
21 Bhandari, Y. R. *et al.* Transcription factor expression repertoire basis for epigenetic and transcriptional subtypes of colorectal cancers. *Proceedings of the National Academy of Sciences* **120**, e2301536120 (2023).
22 Jones, P. A. & Baylin, S. B. The epigenomics of cancer. *Cell* **128**, 683-692 (2007).
23 Goltz, D., Gevensleben, H., Dietrich, J. & Dietrich, D. PD-L1 (CD274) promoter methylation predicts survival in colorectal cancer patients. *Oncoimmunology* **6**, e1257454 (2017).
24 Hogg, S. J. *et al.* Targeting histone acetylation dynamics and oncogenic transcription by catalytic P300/CBP inhibition. *Molecular cell* **81**, 2183-2200. e2113 (2021).
25 Zhao, T., Li, Y., Zhang, J. & Zhang, B. PD-L1 expression increased by IFN-γ via JAK2-STAT1 signaling and predicts a poor survival in colorectal cancer. *Oncology letters* **20**, 1127-1134 (2020).
26 Mohammadzadeh, S. *et al.* Producing Soluble Human Programmed Cell Death Protein-1: A Natural supporter for CD4+ T cell Cytotoxicity and Tumor Cells Apoptosis. *Iranian Journal of Biotechnology* **17**, e2104 (2019).
27 Bai, J. *et al.* Regulation of PD-1/PD-L1 pathway and resistance to PD-1/PD-L1 blockade. *Oncotarget* **8**, 110693 (2017).
28 Chen, X. *et al.* Epigenetic strategies synergize with PD-L1/PD-1 targeted cancer immunotherapies to enhance antitumor responses. *Acta Pharmaceutica Sinica B* **10**, 723-733 (2020).
29 Mohammadzadeh, S., Andalib, A., Khanahmad, H. & Esmaeil, N. Human recombinant soluble PD1 can interference in T cells and Treg cells function in response to MDA-MB-231 cancer cell line. *American Journal of Clinical and Experimental Immunology* **12**, 11 (2023).
30 Marasco, M. *et al.* Molecular mechanism of SHP2 activation by PD-1 stimulation. *Science advances* **6**, eaay4458 (2020).
31 Dong, Y., Sun, Q. & Zhang, X. PD-1 and its ligands are important immune checkpoints in cancer. *Oncotarget* **8**, 2171 (2017).
32 Schillebeeckx, I. *et al.* T cell subtype profiling measures exhaustion and predicts anti-PD-1 response. *Scientific reports* **12**, 1342 (2022).

33 Cillo, A. R. *et al.* Blockade of LAG-3 and PD-1 leads to co-expression of cytotoxic and exhaustion gene modules in CD8+ T cells to promote antitumor immunity. *Cell* **187**, 4373-4388. e4315 (2024).

34 Boussiotis, V. A., Chatterjee, P. & Li, L. Biochemical signaling of PD-1 on T cells and its functional implications. *The cancer journal* **20**, 265-271 (2014).

35 Chen, D. S. & Mellman, I. Elements of cancer immunity and the cancer–immune set point. *Nature* **541**, 321-330 (2017).

36 Lin, X. *et al.* Regulatory mechanisms of PD-1/PD-L1 in cancers. *Molecular cancer* **23**, 108 (2024).

37 Zhu, Y.-H. *et al.* Immunosuppression, immune escape, and immunotherapy in pancreatic cancer: focused on the tumor microenvironment. *Cellular Oncology* **46**, 17-48 (2023).

38 Llosa, N. J. *et al.* (American Society of Clinical Oncology, 2014).

39 Vogelstein, B. *et al.* Cancer genome landscapes. *science* **339**, 1546-1558 (2013).

40 Bruni, D., Angell, H. K. & Galon, J. The immune contexture and Immunoscore in cancer prognosis and therapeutic efficacy. *Nature Reviews Cancer* **20**, 662-680 (2020).

41 Du, M., Drew, D. A., Goncalves, M. D., Cao, Y. & Chan, A. T. Early-onset colorectal cancer as an emerging disease of metabolic dysregulation. *Nature Reviews Endocrinology* **21**, 686-702 (2025).

42 Horvath, S. & Raj, K. DNA methylation-based biomarkers and the epigenetic clock theory of ageing. *Nature reviews genetics* **19**, 371-384 (2018).

43 Vaidya, H., Jelinek, J. & Issa, J.-P. J. DNA methylation, aging, and cancer. *Epigenomes* **9**, 18 (2025).

44 Tian, H.-Y., Liu, C.-A. & Shi, H.-P. Association Between Fat Mass Index, Fat Free Mass Index and Metabolic Syndrome, Cachexia, and All-Cause Mortality Among Patients with Cancer. *Nutrition and Cancer* **78**, 123-133 (2026).

45 Wang, F. *et al.* The interplay between tumor-intrinsic KRT6A and host-derived immune-nutritional status (PNI) defines prognosis in resectable PDAC. *Scientific Reports* (2026).

46 Fearon, K. Definition and classification of cancer cachexia. *Palliative Medicine* **26**, 387 (2012).

47 Zhou, T. C. *et al.* in *Urologic Oncology: Seminars and Original Investigations.* 14-20 (Elsevier).

48 Chen, K., Zhu, F., Li, X. & Yoshimura, T. Advances in Immune Checkpoint Inhibitors for Cancer Treatment. *Cancers* **18**, 1804 (2026).

49 Wherry, E. J. & Kurachi, M. Molecular and cellular insights into T cell exhaustion. *Nature Reviews Immunology* **15**, 486-499 (2015).

50 Gu, L.-H. *et al.* Molecular mechanisms and potential targeting strategies of ubiquitin-proteasome system-mediated PD-1/PD-L1 ubiquitination in tumor immune suppression. *Oncology Reports* **54**, 167 (2025).

51 Xie, H. *et al.* NK cell exosomes alleviate PD-l1 expression and facilitate tumor immunity by repressing PI3K-AKT-mTOR signaling. *Immunological Investigations* **54**, 382-395 (2025).

52 Rubin, J. B. *et al.* Epigenetic developmental mechanisms underlying sex differences in cancer. *The Journal of Clinical Investigation* **134** (2024).

53 González-Flores, E. *et al.* Gender and sex differences in colorectal cancer screening, diagnosis and treatment. *Clinical and Translational Oncology*, 1-13 (2025).

54 Tsokkou, S. *et al.* Sex differences in colorectal cancer: Epidemiology, risk factors, and clinical outcomes. *Journal of Clinical Medicine* **14**, 5539 (2025).
55 Ye, Y. *et al.* Sex-associated molecular differences for cancer immunotherapy. *Nature communications* **11**, 1779 (2020).
56 Zhou, X. *et al.* Mucosal immune response in biology, disease prevention and treatment. *Signal transduction and targeted therapy* **10**, 7 (2025).
57 Levra Levron, C. *et al.* Bridging tissue repair and epithelial carcinogenesis: epigenetic memory and field cancerization. *Cell Death & Differentiation* **32**, 78-89 (2025).
58 Dimitrov, L. *et al.* Biomarkers of Common Molecular Dysregulation in Tumor Tissue and Peritumor Mucosa in Head and Neck SCC: Insights into Field Cancerization. *International Journal of Molecular Sciences* **27**, 1212 (2026).
59 Devall, M. A. *et al.* DNA methylation analysis of normal colon organoids from familial adenomatous polyposis patients reveals novel insight into colon cancer development. *Clinical Epigenetics* **14**, 1-11 (2022).
60 Molero, A. *et al.* Assessment of PD-L1 expression and tumour infiltrating lymphocytes in early-stage non-small cell lung carcinoma with artificial intelligence algorithms. *Journal of Clinical Pathology* **78**, 456-464 (2025).

Acknowledgements: This work was supported by Isfahan University of Medical Sciences and Poursina Hakim Digestive Diseases Research Center. The authors gratefully acknowledge the Poursina Hakim Cancer Prevention Association, Isfahan, Iran for its support, collaboration, and assistance during the course of this study. Their contribution is sincerely appreciated.

Authors' contributions: Fatemeh Maghool, Samane Mohammadzadeh1: Conceptualization, methodology, formal analysis, and original draft preparation. Mohammad Hassan Emamei: Supervision, project administration, funding acquisition, and final editing. Parisa Kadkhodaei, Pouria Samadi1, and Safoora Mohammadzadeh: Data curation, investigation, and software application. Razieh Kamali, Alireza Fahim, Elham Amjadi1, Aida Heidari: Validation, visualization, and reviewing the manuscript.

Data Availability: All data generated or analyzed during this study are included in this published article (and its supplementary information files).

Competing interests: The authors declare no potential conflicts of interest.

Figure Legends:

Figure 1. Comparison of methylation or expression levels of PD-1 and PD-L1 genes between normal tissues in the three groups (normal, ACA, and CRC) and between diseased and adjacent normal tissues in the two groups (ACA and CRC). A: Comparison of PD-1 methylation levels, B: Comparison of PD-1 expression levels, C: Comparison of PD-L1 methylation levels and D: Comparison of PD-L1 expression levels. ACA: Advanced Colorectal Adenomas, N.Adj.ACA: ACA-adjacent normal tissues, CRC: Colorectal Cancer, N.Adj.CRC: CRC-adjacent normal tissues, PD-1: Programmed Death-1 protein, PD-L1: Programmed Death-Ligand 1, Meth. H: Methylation site detection by HpaII restriction enzyme, Meth. M: Methylation site detection by MspI restriction enzyme, Meth. Total: Methylation site detection by HpaII and MspI restriction enzymes, Exp.N: Expression compraring normal tissue, Exp.Adj: Expression comparing adjacent normal tissue. $p<0.05$ in: *Normal Vs ACA, # Normal Vs CRC, & ACA Vs CRC, ^ACA Vs N.Adj.ACA, $CRC Vs N.Adj.CRC

Table. 1. Comparison of demographic characteristics among the CRC, ACA, and control (values are presented as number and percentage).

		GROUP: N (%)			P VALUE
		Normal	ACA	CRC	
GENDER	Male	6 (35.3%)	15 (62.5%)	16 (69.6%)	#P=0.052
	Female	11 (64.7%)	9 (37.5%)	7 (30.4%)	-
AGE	<45	2 (22.2%)	6 (66.7%)	1 (11.1%)	-
	45-59	6 (46.2%)	2 (15.4%)	5 (38.5%)	-
	≥60	9 (21.4%)	16 (38.1%)	17 (40.5%)	-
BMI	<25	3 (11.5%)	11 (42.3%)	12 (46.2%)	#P=0.027
	≥25	14 (36.8%)	13 (34.2%)	11 (28.9%)	-
SMOKING	Smoker	15 (33.3%)	15 (33.3%)	15 (33.3%)	-
	No Smoker	0 (0.0%)	5 (50%)	5 (50%)	-
	Former Smoker	2 (22.2%)	4 (44.4%)	3 (33.3%)	-

ACA: Advanced Colorectal Adenomas, CRC: Colorectal Cancer, BMI: Body Mass Index
$p<0.05$ in: *Normal Vs ACA, # Normal Vs CRC, & ACA Vs CRC

Table.2. Comparison of PD-1 and PD-L1 expression and methylation between females and males in healthy individuals, patients with ACA, and patients with tumors.

		NORMAL						ACA						CRC						
GENDER		Male			Female			Male			Female			Male			Female			P VALUE
		N	Mean	Std. Deviation	N	Mean	Std. Deviation	N	Mean	Std. Deviation	N	Mean	Std. Deviation	N	Mean	Std. Deviation	N	Mean	Std. Deviation	
PD-1	Meth.H	4	312.74	167.31	6.00	227.29	108.80	11	269.93	98.91	4.00	198.70	136.12	8	302.49	208.24	5.00	286.42	118.28	-
	Meth.M	4	372.24	228.99	6.00	205.55	73.13	11	272.00	161.95	4.00	154.11	101.99	8	266.31	144.79	5.00	250.21	207.30	-
	Meth. Total	4	342.49	167.22	6.00	216.42	67.77	11	270.97	118.99	4.00	176.40	117.70	8	284.40	155.33	5.00	268.31	158.81	-
	Exp. N	5	0.90	0.47	5.00	1.24	0.21	8	0.72	0.23	2.00	0.76	0.06	9	0.57	0.27	1.00	0.84		-
	exp.Adj	5	0.90	0.47	5.00	1.24	0.21	8	0.73	0.23	2.00	0.76	0.07	9	0.56	0.26	1.00	0.83		-
PD-L1	Meth.H	3	200.27	126.02	7.00	209.66	132.41	15	99.48	83.44	8.00	85.15	8.71	5	19.25	5.67	4.00	10.78	3.83	-
	L1. Meth. M	3	272.65	106.03	7.00	285.20	288.02	15	124.71	170.43	8.00	93.96	28.42	5	15.15	6.15	4.00	17.02	6.21	-
	Meth. Total	3	236.46	59.80	7.00	247.43	183.44	15	112.10	126.85	8.00	89.55	15.91	5	17.20	4.70	4.00	13.90	2.80	-
	Exp. N	5	0.92	0.28	5.00	1.14	0.17	8	0.80	0.29	2.00	1.09	0.03	9	1.21	0.27	1.00	1.72		#P=0.01
	Exp. Adj	5	0.92	0.28	5.00	1.14	0.17	8	1.28	0.46	2.00	1.74	0.04	9	7.26	1.62	1.00	10.29		#P=0.01

ACA: Advanced Colorectal Adenomas, CRC: Colorectal Cancer, PD-1: Programmed Death-1 protein, PD-L1: Programmed Death-Ligand 1, Meth.H: Methylation site detection by HpaII restriction enzyme, Meth.M: Methylation site detection by MspI restriction enzyme, Meth.total: Methylation site detection by HpaII and MspI restriction enzymes, Exp.N: Expression compraring normal tissue, Exp.Adj: Expression comparing adjacent normal tissue. $p<0.05$ in: # ACA, between Famale and Male.

Table.3. Pearson Correlation between PD-L1 expression and PD-1 expression in Normal, ACA, CRC tissues and Adjacent normal tissues of ACA and CRC tissue.

			PD-L1	
GROUPS			Exp. N	Exp. Adj
NORMAL	**PD-1**	Exp. N (n=10)	.750*	.750*
		Exp. Adj (n=10)	.750*	.750*
ACA		Exp. N (n=10)	.419	.419
		Exp. Adj (n=10)	.419	.419
CRC		Exp. N (n=10)	.072	.072
		Exp. Adj (n=10)	.072	.072
N.ADJA.ACA		Exp. N (n=11)	-.116	-.116
		Exp. Adj (n=11)	-.112	-.112
N.ADJA.CRC		Exp. N (n=9)	-.556	-.556
		PD-1. Exp. Adj (n=9)	-.556	-.556

ACA: Advanced Colorectal Adenomas, N.Adj.ACA: ACA-adjacent normal tissues, CRC: Colorectal Cancer, N.Adj.CRC: CRC-adjacent normal tissues, PD-1: Programmed Death-1 protein, PD-L1: Programmed Death-Ligand 1, Exp.N: Expression compraring normal tissue, Exp.Adj: Expression comparing adjacent normal tissue. *P value <0.05.

Table.4. Pearson Correlation between PD-L1 and PD-1methylation in Normal, ACA, CRC tissues and Adjacent normal tissues of ACA and CRC tissue.

			PD-L1		
		Groups	Meth.H	Meth.M	Meth. Total
NORMAL (N=8)	**PD-1**	Meth.H	-.832*	-.196	-.509
		Meth.M	-.501	-.318	-.471
		Meth. Total	-.844*	-.304	-.602
ACA (N=14)		Meth.H	.171	.138	.149
		Meth.M	.282	.284	.284
		Meth. Total	.254	.241	.246
CRC (N=8)		Meth.H	.040	.320	.224
		Meth.M	.599	.550	.766*
		Meth. Total	.295	.480	.505
N.ADJA.ACA (N=13)		Meth.H	.336	.432	.407
		Meth.M	.498*	.734**	.656*
		Meth. Total	.445	.626*	.570*
N.ADJA.CRC (N=8)		Meth.H	.543	.543	.543
		Meth.M	.395	.396	.395
		Meth. Total	.500	.501	.500

ACA: Advanced Colorectal Adenomas, N.Adj.ACA: ACA-adjacent normal tissues, CRC: Colorectal Cancer, N.Adj.CRC: CRC-adjacent normal tissues, PD-1: Programmed Death-1 protein, PD-L1: Programmed Death-Ligand 1, Meth. H: Methylation site detection by HpaII restriction enzyme, Meth. M: Methylation site detection by MspI restriction enzyme, Meth. Total: Methylation site detection by HpaII and MspI restriction enzymes, *P value <0.05, **P value <0.005.

Table 5. Primer sequences designed for amplifing genomic regions flanking informative MSRE recognition sites

GENE	DIRECTION	SEQUENCE (5′→3′)
PD-L1	Forward	AGGTCAGGAAAGTCCAACGC
	Reverse	GAGGAACAACGCTCCCTACC
PD-1	Forward	TTTGAGGGGGAGCCGATTAG
	Reverse	CAACCCCACTCCCATTCTGTC

Table 6. Primer sequences designed for quantification of gene expression analysis

GENE	DIRECTION	PRIMER
PD. L1 **(RT)**	Forward	CCCCATACAACAAAATCAACCA
	Reverse	TGCTTGTCCAGATGACTTCG
PD-1 **(RT)**	Forward	CCAAGGCGCAGATCAAAGAGA
	Reverse	TGGGCTGTGGGCACT
ACTB	Forward	AGAGCTACGAGCTGCCTGAC
	Reverse	AGCACTGTGTTGGCGTACAG

Supplementary Table.1. Pearson Correlation between methylation and expression of PD-1 or PD-L1 genes in Normal, ACA, CRC tissues and Adjacent normal tissues of ACA and CRC tissue.

		PD-1			PD-L1		
GROUPS		Meth.H	Meth.M	Meth. Total	Meth.H	Meth.M	Meth. Total
NORMAL	Exp. N	.895	.051	.445	-.807	.536	-.176
	Exp. Adj	.895	.051	.445	-.807	.536	-.176
ACA	Exp. N	.186	.115	.145	-.077	.251	.186
	Exp. Adj	.186	.115	.145	-.077	.251	.186
CRC	Exp. N	.159	.472	.333	-.226	.856	.508
	Exp. Adj	.159	.472	.333	-.226	.856	.508
N.ADJA.ACA	Exp. N	.658	.969**	.844*	-.351	-.485	-.442
	Exp. Adj	.658	.969**	.844*	-.351	-.485	-.442
N.ADJA.CRC	Exp. N	.868*	.643	.804*	-.435	-.423	-.429
	Exp. Adj	.868*	.643	.804*	-.435	-.423	-.429

ACA: Advanced Colorectal Adenomas, N.Adj.ACA: ACA-adjacent normal tissues, CRC: Colorectal Cancer, N.Adj.CRC: CRC-adjacent normal tissues, PD-1: Programmed Death-1 protein, PD-L1: Programmed Death-Ligand 1, Meth. H: Methylation site detection by HpaII restriction enzyme, Meth. M: Methylation site detection by MspI restriction enzyme, Meth. Total: Methylation site detection by HpaII and MspI restriction enzymes, Exp.N: Expression compraring normal tissue, Exp.Adj: Expression comparing adjacent normal tissue. *P value <0.05, **P value <0.005.

Supplementary Table 2. Correlation coefficient between PD-L1 and PD-1 methylation and expression levels with TIL density in ACA tissue

	PD-1. METH. H	PD-1. METH. M	PD-1. METH. TOTAL	PD-1. EXP. N	PD-1. EXP. ADJ	PD-L1. METH. H	PD-L1. METH. M	PD-L1. METH. TOTAL	PD-L1. EXP. N	PD-L1. EXP. ADJ
TIL	0.586*	0.417	0.482	-0.062	-0.062	-0.322	-0.157	-0.210	-0.209	-0.209
N	13	13	13	10	10	22	22	22	10	10

ACA: Advanced Colorectal Adenomas, N.Adj.ACA: ACA-adjacent normal tissues, CRC: Colorectal Cancer, N.Adj.CRC: CRC-adjacent normal tissues, PD-1: Programmed Death-1 protein, PD-L1: Programmed Death-Ligand 1, Meth. H: Methylation site detection by HpaII restriction enzyme, Meth. M: Methylation site detection by MspI restriction enzyme, Meth. Total: Methylation site detection by HpaII and MspI restriction enzymes, Exp.N: Expression compraring normal tissue, Exp.Adj: Expression comparing adjacent normal tissue. TIL: Tumor-infiltrating lymphocyte. *P value <0.05

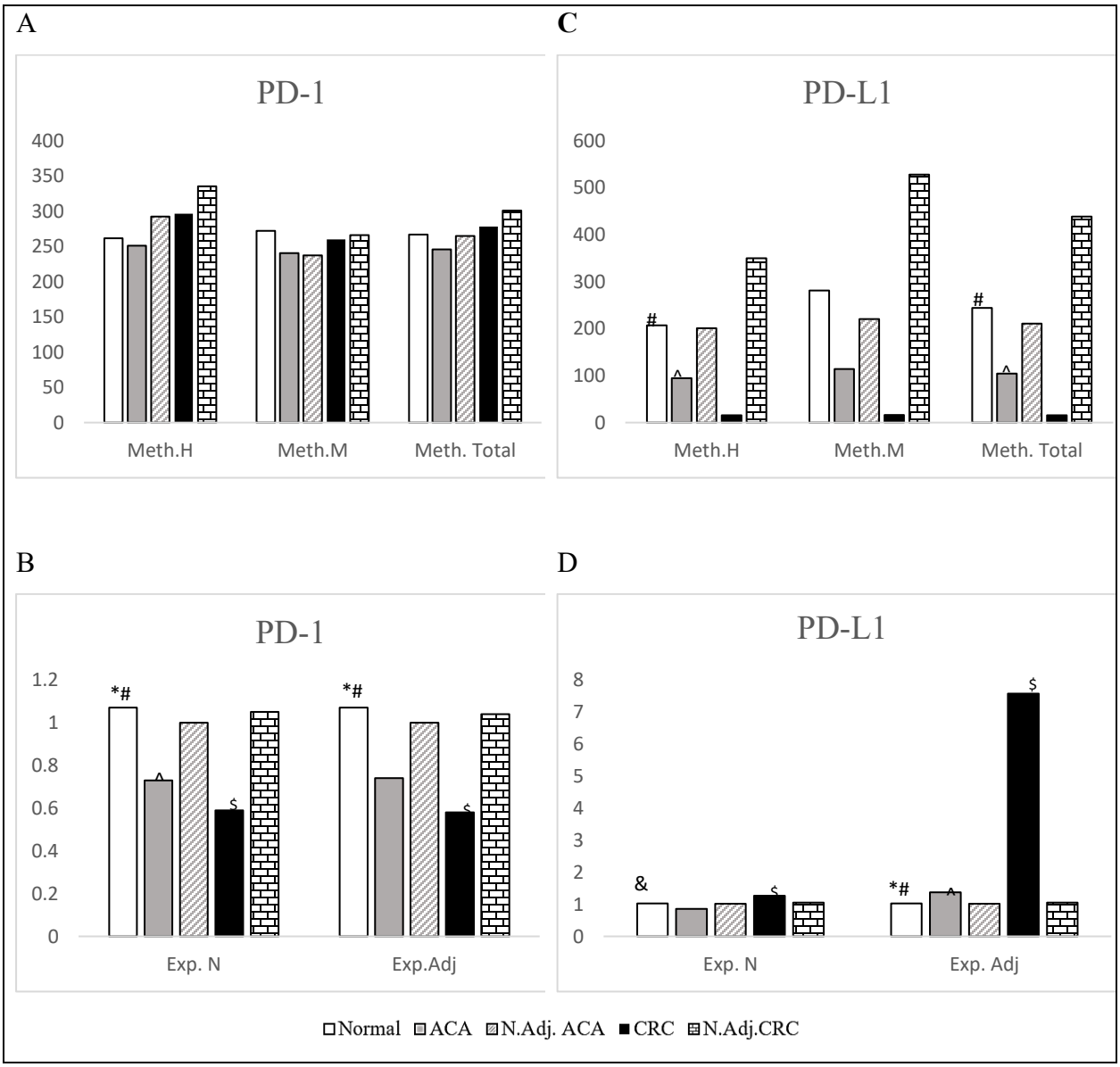


Figure 1. Comparison of methylation or expression levels of PD-1 and PD-L1 genes between normal tissues in the three groups (normal, ACA, and CRC) and between diseased and adjacent normal tissues in the two groups (ACA and CRC). A: Comparison of PD-1 methylation levels, B: Comparison of PD-1 expression levels, C: Comparison of PD-L1 methylation levels and D: Comparison of PD-L1 expression levels. ACA: Advanced Colorectal Adenomas, N.Adj.ACA: ACA-adjacent normal tissues, CRC: Colorectal Cancer, N.Adj.CRC: CRC-adjacent normal tissues, PD-1: Programmed Death-1 protein, PD-L1: Programmed Death-Ligand 1, Meth. H: Methylation site detection by HpaII restriction enzyme, Meth. M: Methylation site detection by MspI restriction enzyme, Meth. Total: Methylation site detection by HpaII and MspI restriction enzymes, Exp.N: Expression compraring normal tissue, Exp.Adj: Expression comparing adjacent normal tissue. $p<0.05$ in: *Normal Vs ACA, # Normal Vs CRC, & ACA Vs CRC, ^ACA Vs N.Adj.ACA, $CRC Vs N.Adj.CRC